^{124}I-huA33 Antibody PET of Colorectal Cancer

Jorge A. Carrasquillo[1], Neeta Pandit-Taskar[1], Joseph A. O'Donoghue[2], John L. Humm[2], Pat Zanzonico[2], Peter M. Smith-Jones[1], Chaitanya R. Divgi[1], Daniel A. Pryma[1], Shutian Ruan[1], Nancy E. Kemeny[3], Yuman Fong[4], Douglas Wong[4], Jaspreet S. Jaggi[5], David A. Scheinberg[5], Mithat Gonen[6], Katherine S. Panageas[6], Gerd Ritter[5,7], Achim A. Jungbluth[5,7], Lloyd J. Old[5,7], and Steven M. Larson[1]

[1]Nuclear Medicine Service, Department of Radiology, Memorial Sloan-Kettering Cancer Center, New York, New York; [2]Department of Medical Physics, Memorial Sloan-Kettering Cancer Center, New York, New York; [3]Department of Medicine, Memorial Sloan-Kettering Cancer Center, New York, New York; [4]Department of Surgery, Memorial Sloan-Kettering Cancer Center, New York, New York; [5]Sloan-Kettering Institute, Memorial Sloan-Kettering Cancer Center, New York, New York; [6]Biostatics Branch, Memorial Sloan-Kettering Cancer Center, New York, New York; and [7]New York Branch of the Ludwig Institute for Cancer Research, Memorial Sloan-Kettering Cancer Center, New York, New York

Humanized A33 (huA33) is a promising monoclonal antibody that recognizes A33 antigen, which is present in more than 95% of colorectal cancers and in normal bowel. In this study, we took advantage of quantitative PET to evaluate ^{124}I huA33 targeting, biodistribution, and safety in patients with colorectal cancer. We also determined the biodistribution of ^{124}I-huA33 when a large dose of human intravenous IgG (IVIG) was administered to manipulate the Fc receptor or when ^{124}I-huA33 was given via hepatic arterial infusion (HAI). **Methods:** We studied 25 patients with primary or metastatic colorectal cancer; 19 patients had surgical exploration or resection. Patients received a median of 343 MBq (44.4–396 MBq) and 10 mg of ^{124}I-huA33. Nineteen patients received the antibody intravenously and 6 patients via HAI, and 5 patients also received IVIG. **Results**: Ten of 12 primary tumors were visualized in 11 patients. The median concentration in primary colon tumors was 0.016% injected dose per gram, compared with 0.004% in normal colon. The PET-based median ratio of hepatic tumor uptake to normal-liver uptake was 3.9 (range, 1.8–22.2). Quantitation using PET, compared with well counting of serum and tissue, showed little difference. Prominent uptake in bowel hindered tumor identification in some patients. Pharmacokinetics showed that patients receiving IVIG had a significantly shorter serum half-time (41.6 ± 14.0 h) than those without (65.2 ± 9.8 h). There were no differences in clearance rates among the intravenous group, IVIG group, and HAI group, nor was there any difference in serum area under the curve, maximum serum concentration, or volume of distribution. Weak titers of human–anti-human antibodies were observed in 6 of 25 patients. No acute side effects or significant toxicities were associated with huA33. **Conclusion:** Good localization of ^{124}I-huA33 in colorectal cancer with no significant toxicity has been observed. PET-derived ^{124}I concentrations agreed well with those obtained by well counting of surgically resected tissue and blood, confirming the quantitative accuracy of ^{124}I-huA33 PET. The HAI route had no advantage over the intravenous route. No clinically significant changes in blood clearance were induced by IVIG.

Key Words: A33; ^{124}I, antibody; arterial; positron; colon

J Nucl Med 2011; 52:1173–1180

DOI: 10.2967/jnumed.110.086165

Radiolabeled monoclonal antibodies (mAbs) have been approved for tumor imaging as part of a therapeutic regimen (ibritumomab or tositumomab) or as stand-alone diagnostic reagents, as well as nonradiolabeled therapeutic reagents (*1*). Several of the radiolabeled mAbs are no longer available (arcitumomab, satumomab) because of limited sensitivity for tumor detection or because of better imaging modalities, such as ^{18}F-FDG PET. However, radiolabeled mAbs may have significantly greater specificity than ^{18}F-FDG and allow for quantitation of tumor antigens—potentially important in selecting therapy or evaluating response. Most radiolabeled mAbs have been labeled with single-photon emitters. PET has many advantages over SPECT, including superior sensitivity, resolution, contrast, and quantitative accuracy, as illustrated by the mAbs ^{124}I-cG250 and ^{89}Zr-trastuzumab (*2,3*).

A33 is a transmembrane glycoprotein that has homology to tight junction–associated proteins and is present in normal colon and small-bowel epithelium, over 95% of human colon adenocarcinomas, and approximately 50% of gastric and pancreatic cancers although absent from most other human tissues and tumors (*4*). Recent studies have shown that A33 does not internalize when bound by A33 mAb (*5*), a finding that may explain the prolonged retention of A33 mAb in tumors (*6*). Prior studies with murine A33 have shown its safety, tumor-targeting ability, and specificity (*6–8*). Trials with humanized A33 (huA33) mAb alone or combined with chemotherapy have shown favorable tolerability and some evidence of tumor response (*9,10*) and a lower incidence of immune response than with murine A33 (*10–12*).

The longer circulation times of intact IgG than of smaller, more rapidly cleared antibody fragments, although

Received Dec. 3, 2010; revision accepted Feb. 23, 2011.

For correspondence or reprints contact: Jorge Carrasquillo, Memorial Sloan-Kettering Cancer Center, 1275 York Ave., New York, NY 10065.

E-mail: carrasj1@mskcc.org

contributing to higher tumor uptake, also result in higher background levels and greater bone marrow radiation exposure. Patients undergoing ^{131}I-huA33 radioimmunotherapy had longer serum retention of huA33 than of murine A33, and the maximum tolerated dose was 1,480 MBq/m^2, compared with 2,775 MBq/m^2 for murine A33, likely related to the longer serum half-life of ^{131}I-huA33 (*11,13*). It would be desirable if, once sufficient targeting were achieved, clearance of circulating radioactivity could be accelerated. Various approaches attempting to improve tumor-to-nontumor targeting have been evaluated, including multistep strategies or the use of clearing agents (*14–16*). Fc receptor is a complex class I–like protein that plays a central role in perinatal IgG transfer and protection of IgG from catabolism (*17*). We have previously reported, in mice, that high-dose human IgG blocked the neonatal Fc receptor (*18*), resulting in faster blood and whole-body pharmacokinetics and better tumor-to-blood ratios without adversely affecting tumor uptake. In the current study, we translated this approach to the clinic.

The route of administration of antibodies has an important effect on their biodistribution, and studies have shown potential benefits of alternate routes (*19,20*). The advantage of hepatic arterial infusion (HAI) of any pharmaceutical is dependent on the degree of first-pass extraction fraction. Although theoretic data are available to suggest a low extraction fraction from intraarterially administered antibodies, limited clinical data exist for HAI of mAbs and none for huA33. Fan et al. administered iodinated mAb to patients with hepatoma through HAI and concluded that it was superior to intravenous injection, with tumor-to-liver ratios of 1.74 ± 0.57 and 1.34 ± 0.29, respectively (*21*). A trial using HAI of ^{131}I-metuximab, directed against hepatoma, found that it was safe and active (*22*). The same group has also safely administered ^{131}I-hepama mAb via HAI with hepatic artery ligation in patients with hepatoma (*23*) and concluded that this approach may be helpful. Given that hepatic metastases are a major problem in colorectal cancer and that huA33 has a high affinity for its antigen (*24*), we explored whether HAI would result in higher tumor uptake than that of the intravenous injection. Preclinical studies directly comparing the intravenous and HAI routes in a brain tumor model have shown a 20% improvement in delivery via the intraarterial route (*25*), and clinical trials have also been performed (*26*). Thus, in a subset of patients we evaluated the delivery of ^{124}I-huA33 via HAI.

The primary objectives of this study were to evaluate the safety of a single dose of ^{124}I-huA33 and its ability to target colorectal cancer. Secondary objectives included determining the immunogenicity of a single injection of ^{124}I-huA33 and the pharmacokinetics and quantitative imaging characteristics of ^{124}I-huA33 administered through HAI or in conjunction with intravenous IgG (IVIG).

MATERIALS AND METHODS

A33 Antibody and Radiolabeling

HuA33 is a fully humanized IgG1 mAb derived from murine A33 (*24*). The characterization and antigen recognition have been previously described (*27,28*). The huA33 antibody was produced at the Ludwig Institute for Cancer Research and was labeled with ^{124}I using the IODOGEN (Thermo Fisher Scientific) method in accordance with our Investigational New Drug application. Formulations of between 44.4 MBq of ^{124}I/10 mg of A33 and 370 MBq of ^{124}I/10 mg of A33 were produced under current good-manufacturing-practice conditions. In brief, a 30%–40% excess of ^{124}I was incubated with huA33 in an IODOGEN tube. The mixture was purified through an anion exchange column followed by terminal sterilization through a 0.22-μm filter. The activity of the final product was assayed in a dose calibrator, and cold antibody was added to yield a dose containing 10 mg. All products passed pyrogen and sterility testing. The median radiochemical yield was 86% (range, 56%–99%); the median radiochemical purity was 98.2% (range, 91%–100%); and the median immunoreactivity as determined by a cell-binding assay using SW1222 cells was 89% (range, 80%–98%) (*29*).

Patient Eligibility and Protocol Design

Patients were enrolled in an open-label prospective protocol approved by the Institutional Review Board of Memorial Sloan-Kettering Cancer Center. The objectives were to determine the safety, tolerability, pharmacokinetics, biodistribution, tumor-targeting ability, and human–antihuman antibody (HAHA) immune response of ^{124}I-huA33 administered intravenously. Furthermore, we evaluated whether administration of large amounts of IVIG increased the blood clearance of ^{124}I-huA33 and whether localization in liver metastases was better with HAI than with intravenous administration.

The patients had histologically confirmed primary or metastatic colorectal cancer and were candidates for laparotomy for tumor resection or were nonsurgical candidates with liver metastasis larger than 2.5 cm. Other criteria included an expected survival of more than 3 mo, age greater than 18 y, Karnofsky performance status of at least 70, platelet count of at least 75,000/μL, absolute neutrophil count of at least 1,500/μL, white blood cell count of at least 3,000/μL, serum bilirubin level of no more than 2.5 mg/dL, serum creatinine level of no more than 2.0 mg/dL, no clinically significant heart disease, no brain metastasis, and no chemotherapy within 4 wk of the study. All patients provided informed consent.

Twenty-five patients (19 men and 6 women) were imaged. Their median age was 61 y (range, 49–77 y). Each received a single intravenous (n = 19) or HAI (n = 6) administration of ^{124}I-huA33. The antibody was infused intravenously over 5–20 min (19 patients), intraarterially over approximately 5 min (5 patients), or intraarterially over 60 min (1 patient), through a hepatic infusion pump (Codman) previously used for chemotherapy.

Patients scheduled for surgery underwent ^{124}I-huA33 PET the morning of their surgery. In the 19 patients who underwent surgery, the PET results could be correlated with the surgical resection specimen; the 6 patients who did not undergo surgery had CT correlation only. Fifteen patients who had undergone previous resection of their primary tumor had radiographic findings suggestive of metastatic disease; 10 patients were studied with their primary tumor in situ. When tissue could be spared at the time of surgery (16/19 patients), it was weighed and counted in a well

counter, and the percentage injected dose (%ID) of ^{124}I per gram of tumor or normal tissue was determined.

Five patients received Gamunex−IVIG (Talecris Biotherapeutics Inc.), 1 g/kg, 1–2 d after intravenous injection of ^{124}I-huA33. A median of 70.8 g of IVIG (range, 53–90.7 g) in a median of 1.32 L was administered over 5–9 h. All these patients underwent scanning immediately before the start of IVIG and shortly after the end of IVIG (median, 8.6 h after the start of IVIG).

Imaging

Patients were imaged either on an Advance (n = 2; GE Healthcare), Discovery LS (n = 14; GE Healthcare), or DSTE (n = 9; GE Healthcare) PET/CT scanner in 2-dimensional mode with attenuation, scatter, and other standard corrections applied. Images were acquired at 6 min per field of view and included whole-torso imaging from neck to proximal thighs in 14 patients and from mid chest to pelvis in the remainder. All patients underwent their final scan at a median of 8.9 d (range, 4.9–8.9 d) after tracer administration. In addition, 20 patients underwent imaging shortly (median, 2.6 h) after antibody administration, and 14 were imaged at 1 intermediate time point (median, 2 d) between injection and their last scan.

Images were read by an experienced nuclear medicine physician who was aware of the patient's history and diagnostic CT scan report. Localization of tracer in tumor was defined as focal accumulation greater than adjacent background activity in areas where physiologic activity is not expected. Because ^{124}I-huA33 localizes in small bowel and colon, activity in bowel was considered positive for tumor when there was a focal accumulation greater than activity in the adjacent colon. All images and maximum-intensity-projection images were reviewed on a dedicated PET workstation (AW Suite; GE Healthcare). Regions of interest were placed visually over structures of interest, and mean standardized uptake value (SUV) and maximum SUV (SUVmax) normalized to body weight [(kBq/mL activity in region)/(kBq injected activity/body mass in g)] were determined for blood pool, liver, spleen, bowel, thyroid, and small and large bowel. To determine the %ID/g from the PET image, the SUV was divided by the body weight (in g) and multiplied by 100.

Pharmacokinetics

Pharmacokinetic analysis was performed on all patients by drawing blood at approximately 5, 15, 60, and 120 min after antibody administration and on the last day of imaging or surgery (5–9 d). Starting with patient 12, an intermediate blood sample was drawn at 24–72 h after infusion, and in those patients undergoing IVIG infusion, a sample was also drawn immediately before and after IVIG infusion. All samples were centrifuged; serum was divided into aliquots, weighed, and counted in the scintillation well counter with a standard of the injected dose; and the decay-corrected %ID/L in serum was calculated. The data were fit to a monoexponential function because of the limited samples (Prism; GraphPad). The data were used to determine the serum half-time ($T_{1/2}$), volume of distribution, area underneath the curve (AUC), and clearance. The AUC was determined by trapezoidal integration up to the time of the last blood sampling, and the terminal component was estimated using the fitted half-life. To determine the %ID in the plasma volume, the %ID/L at the end of infusion was multiplied by the patient's estimated plasma volume as determined from a nomogram. To determine whether the blood-pool concentration, derived from PET, correlated with counting of serum samples, a region of interest was drawn over the atrial blood pool. The SUVmax in the blood was converted to %ID/L of serum using the patient's hematocrit level.

To determine whether IVIG accelerated the blood clearance of ^{124}I-huA33, we compared the AUC and $T_{1/2}$ of those patients receiving and not receiving IVIG. Further, we compared the activity in the last serum sample measured in those patients receiving IVIG with that of other patients, who had similarly timed serum activity measurements but did not receive IVIG. We also compared the observed and expected immediate post-IVIG serum concentrations by extrapolating the clearance from the pre-IVIG serum sample using the mean $T_{1/2}$ determined from those patients not receiving IVIG and accounting for the time elapsed between the pre- and post-IVIG samples. The SUVmax in pre-IVIG liver, spleen, bowel, and kidney regions of interest was compared with that after IVIG administration to assess the effect of the IVIG on ^{124}I-huA33 biodistribution.

Evaluation for Toxicity

Patients were monitored for adverse events during the infusion, at each imaging visit, and at 35 ± 3 d after infusion. Adverse events were graded using the National Cancer Institute toxicity criteria (*30*).

Evaluation for HAHA

The patients' serum was evaluated for HAHA before injection and at an approximate mean of 39 ± 19 d after infusion. The HAHA assay was performed by surface plasmon resonance technology using a BIACORE 2000 instrument (GE Healthcare) as previously described (*31*).

Statistics

Descriptive statistics include median or mean ± SD. Because of the small sample sizes, nonparametric methods were used for group comparisons: Wilcoxon signed rank for paired comparisons and Kruskal–Wallis 1-way ANOVA for comparisons across 3 groups. All statistical analyses were performed with SigmaStat 3.5 (Systat Software Inc.).

RESULTS

Patients and Dosing

Patients received a median dose of 343 MBq (range, 44.4–396 MBq) of ^{124}I-huA33 with a total of 10 mg of huA33. No toxicity or adverse side effects attributable to the huA33 were observed. HAHA was not present in any of the preinjection baseline serum, although low titers developed in 6 of the 25 patients.

Imaging Results

Individual conventional imaging results, ^{124}I-huA33 imaging results, and surgical findings are presented in Supplemental Table 1 (supplemental materials are available online only at http://jnm.snmjournals.org). Eleven patients had 12 primary tumors in situ. Ten of these 12 primaries were positive for ^{124}I-huA33 uptake. One of the 2 primary colon tumors negative for uptake was in a patient with prior adjuvant chemotherapy and a negative ^{18}F-FDG PET result at the time of ^{124}I-huA33 imaging. In all 10 patients with liver metastases, the metastases were detected by ^{124}I-huA33 (Supplemental Table 1; Figs. 1 and 2). In 4 of 7

patients with nodal metastases, the ^{124}I-huA33 scan was positive for uptake; 2 of the PET-negative nodal sites were identified only at surgery. Lung lesions in 2 of 5 patients were positive for uptake on PET.

Tissue Uptake

Based on well counting of tissue biopsy specimens from patients receiving intravenous ^{124}I-huA33 (Table 1), the median concentration was 0.016 %ID/g in primary colon tumors and 0.004 %ID/g in normal colon ($P < 0.001$), with a mean ratio of 4.8 for tumor uptake to normal-colon uptake (range, 2.5–8.6). Three of the 5 patients positive for liver lesions at surgery had liver tumor specimens available for counting; these had a median concentration of 0.004 %ID/g, compared with 0.001 %ID/g in normal adjacent liver, resulting in a median ratio of 3.9 for tumor uptake to normal-liver uptake (range, 1.8–22.2). The range of concentration in 3 normal ileum specimens was 0.003–0.007 %ID/g.

When the concentration in normal colon and liver biopsy samples was measured with the well counter and compared with that determined by PET ($n = 12$), there was no significant difference between mean well-counting and PET-derived concentrations: 0.0033 ± 0.002 and 0.0032 ± 0.0039 %ID/g ($P = 0.23$), respectively. The mean concentration in colon and liver tumor specimens determined by well counting, 0.017 ± 0.011 %ID/g, was significantly higher than that based on PET, 0.010 ± 0.004 %ID/g ($P = 0.019$); however, these values correlated with each other (Pearson correlation coefficient, 0.646). There were 10 patients with PET-positive liver lesions, with a ratio of 9.3 ± 6.1 for metastasis uptake to normal-liver uptake and a mean concentration of 0.0096 ± 0.004 %ID/g in lesions.

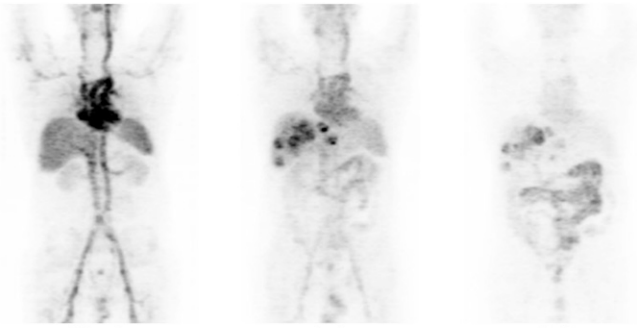

FIGURE 1. Patient 18, with colorectal cancer metastatic to liver. Maximum-intensity-projection images were obtained after HAI infusion of 361.4 MBq of ^{124}I-huA33. Images are scaled to same maximum. Initial image at 45 min shows predominant blood-pool activity. Two-day image shows some clearing from blood pool, excellent localization in liver lesions (SUVmax, 11.2), and some uptake in bowel. At 7 d, there is persistent uptake in liver lesions (SUVmax, 11.2), prominent bowel uptake, and significant decrease in blood-pool activity.

The concentrations in serum, based on the early postinjection and last PET scans, were compared with the well-counting–derived respective values (Fig. 3). Overall, the concentration in serum based on the early whole-body PET scan was 12% less than that based on well counting: 28.1 ± 6.2 and 31.8 ± 7.3 %ID/L ($P = 0.043$), respectively. There was no significant difference in serum concentrations at the late time point: 6.9 ± 3.5 and 6.1 ± 2.2 %ID/L for PET and well counting, respectively ($P = 0.105$).

Early imaging, performed at a median of 2.6 h and maximum of 4.8 h after injection, showed predominantly blood-pool activity (Fig. 1), and in only 1 patient was tumor visualized in the early images. To assess the huA33 kinetics in tumor by PET, the SUVmax at the intermediate imaging time point (47.7 ± 21.9 h from injection) was compared with that at the last imaging time point (187.6 ± 51.0 h from injection). Seventeen tumors (13 patients) were visualized on both the intermediate and the late scans, which were obtained a mean of 139.9 ± 58.4 h apart. In 3 tumors, there was either no change or an increase in tumor uptake between the 2 scans. In the other 14 tumors, there was some decrease in uptake, corresponding to a mean biologic $T_{1/2}$ of 336 h when fit to a monoexponential function.

In addition, the intermediate images always showed prominent uptake in small bowel (Fig. 1), with a mean SUVmax of 12.8 and 11.7 at the intermediate and late time points, respectively ($n = 14$). In 7 patients, the small-bowel uptake increased from the intermediate image to the late image; in the other 7, there was a decrease with a mean $T_{1/2}$ of 394 h. Furthermore, uptake in colon was less prominent than in small bowel, with a mean SUVmax of 3.2 and 3.3 at the intermediate and late time points, respectively. In 7 patients, uptake in colon increased slightly, whereas in 6 patients it decreased with a mean $T_{1/2}$ of 443 h.

Pharmacokinetics

The pharmacokinetic parameters for the 3 groups—intravenous, IVIG, and HAI—are shown in Table 2. With the exception of the shorter $T_{1/2}$ for the IVIG group than for the other groups, there were no significant differences in any pharmacokinetic parameters. On the basis of the well counting–derived %ID/L at the initial time point after injection, most of the activity (97 ± 17 %ID) was still in circulation at that time.

Effect of IVIG and HAI

The plasma concentration after the IVIG infusion at 9 ± 2 h dropped a mean of 21% ± 4% from the value present on the pre-IVIG concentration. In comparison, the expected decrease based on the monoexponential function fitted to the plasma time–activity data for patients not receiving IVIG was only 9% ± 4%.

In 4 patients, the mean %ID drop in serum after IVIG was expressed as a fraction of their initial serum concentration. The concentration after IVIG decreased to a mean of 36.5% of the initial value at a mean of 49.8 h after

RGB

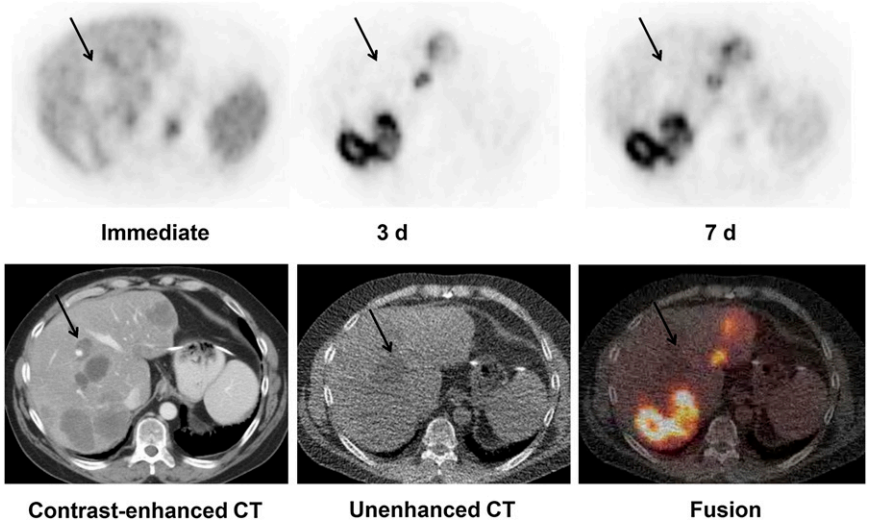

FIGURE 2. Patient 19, with colorectal cancer metastatic to liver. Patient received HAI of 368 MBq of ^{124}I-huA33. Initial images show blood-pool activity, with foci of uptake in liver that appear as cold defects. At 3 d and 7 d, there is marked and persistent localization of uptake in known liver metastasis. Cold defects represent bilomas (arrows) that persisted as non–antibody-avid.

^{124}I-huA33 infusion (immediately after IVIG). That was a statistically significant decline ($P = 0.005$, paired t test) from their pre-IVIG level. Four patients who did not receive IVIG underwent serum sampling at a comparable time (mean, 46.3 h) after ^{124}I-huA33 infusion and showed a larger mean retention of activity: 57.8% of the initial value. This decrease in serum concentration in the group receiving IVIG was significantly greater than that in the non-IVIG group ($P \leq 0.006$, t test). No redistribution of ^{124}I-huA33 was seen into liver, spleen, kidneys, small bowel, or large bowel after IVIG. Instead, there was a decrease ranging from 5% to 34%.

HAI had no detectable advantage over the intravenous route of administration. Visual comparison of the images at the end of HAI and for intravenous administration did not reveal any differences in biodistribution. Likewise, the pharmacokinetic analysis did not show any significant differences between the HAI and intravenous routes of administration. No tumor targeting was seen in the initial PET images for either route.

DISCUSSION

This study showed that ^{124}I-huA33 could be given safely, with no significant toxicity, by intravenous administration or HAI. The low-titer HAHA that was observed is of unclear significance if repeated dosing were to be performed (*31*). Furthermore, ^{124}I-huA33 showed high uptake in lesions, sufficient for tumor visualization by PET in almost all patients (Supplemental Table 1). PET findings were corroborated by analysis of surgical specimens (Table 1). In addition, imaging confirmed prolonged tumor retention, with a mean biologic $T_{1/2}$ of 336 ± 258 h. In some cases, retention was so long that it was not possible to determine the biologic clearance.

Previous imaging studies with A33 have used single-photon emitters (*11,32*). In contrast, our study was novel in

TABLE 1
Tissue Concentration of Antibody

Patient no.	Tissue	Tumor uptake (%ID/g)	Normal-tissue uptake (%ID/g)	Tumor–to–normal-tissue uptake ratio
1	Colon	0.0106	0.0043	2.5
2	Colon	0.0214	0.00318	6.7
3	Colon	0.0154	0.003757	4.1
4	Colon	0.0167	0.006131	2.7
5	Colon	0.0100	0.001849	5.4
6	Colon	0.0210	0.00244	8.6
7	Colon	0.0260	0.005113	5.1
8	Colon	0.0151	0.003348	3.6
11	Colon	0.0144	0.004548	3.2
15	Colon	0.0420	0.006911	6.1
2	Ileum		0.0049	
3	Ileum		0.0032	
15	Ileum		0.0071	
9	Liver	0.0028	0.0016	1.7
10	Liver	0.0039	0.0010	3.8
15	Liver	0.0288	0.0013	22.1

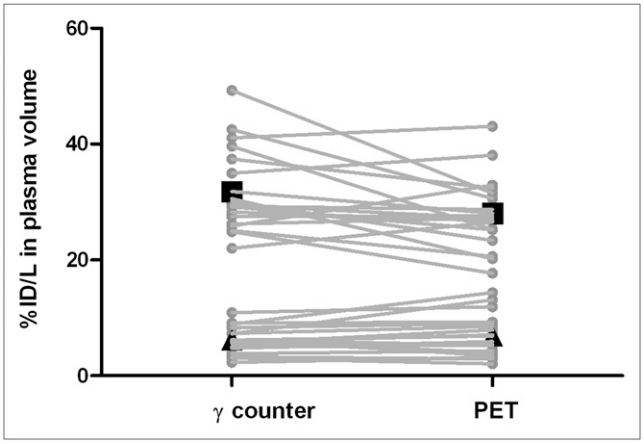

FIGURE 3. Plasma concentration of ^{124}I-huA33 determined by well counting, compared with that estimated from region of interest over blood pool from PET scans. Individual patient samples are plotted, with line connecting values for each patient. Upper family of lines (n = 18) represents early postinjection time, and lower family (n = 20) represents last (presurgical) imaging time. At earliest time after injection, mean concentration in plasma by well counter was 31.8 %ID/L, whereas concentration estimate based on PET was slightly lower, at 28.1 %ID/L (P = 0.0270). At late time, concentration in plasma by well counter was 6.2 %ID/L, whereas estimate based on PET was similar, at 6.9 %ID/L (P = 0.124). ■ = mean value immediately after injection. ▲ = mean value at latest time point that was a mean of 6.9 d after injection.

being the first to use ^{124}I-huA33 and was one of the few studies to use positron-emitting mAbs. In this study, we demonstrated that quantitative ^{124}I-huA33 PET provides reliable estimates of tissue concentration. Although some differences between PET and well-counting–derived serum concentrations were observed, overall these differences were small (Fig. 3). Such differences may be due to technical considerations such as partial-volume averaging and inexact correlation between sites of biopsy specimens and region-of-interest analysis.

As in prior studies, the early distribution of antibody was dominated by blood-pool activity, with a distribution volume comparable to the patient's estimated plasma volume. Because of the limited number of imaging time points, the time of peak tumor uptake could not be determined, although tumor uptake was seen at 2 d. PET of liver tumors yielded a mean uptake of 0.0096 ± 0.0041 %ID/g. Although slightly higher than the mean value reported by Scott et al., 0.005 ± 0.003 %ID/g, it was in the same range (0.002–0.011 %ID/g). The median ratio of liver-tumor concentration to normal-liver concentration by PET was 3.9 and was not significantly different from the 5.8 found by Scott et al. (*32*).

Pharmacokinetic analyses for ^{131}I huA33 have been reported by others (*11,12,32*). In our study, the $T_{1/2}$ was in the lower range of those reported previously, possibly because of the fewer data points used for curve fitting in this study. Nonetheless, the maximum concentration, clearance, and AUC were in the same range as found by previous studies, and distribution volume was similar to that reported by Chong et al. (*11,12,32*).

We could not confirm, in our patients, the large decreases in radiolabeled antibody mediated by Fc receptor that were found in mice when IVIG was administered (*18*). Although we found a decrease in serum ^{124}I-huA33 levels after IVIG infusion, this difference was small, and by 1 wk the levels were comparable to those in non-IVIG–treated cohorts. In addition, the AUCs among cohorts were not significantly different (Table 2). Furthermore, we could not exclude that the drop in serum levels of ^{124}I-huA33 after IVIG could have been due in part to a dilutional effect from the 1.3 L of IVIG infused fluid. PET after IVIG did not show the increase of ^{124}I in organs of catabolism that was seen in the mouse model, although the latter determination is limited by the use ^{124}I versus ^{111}In in mouse studies (*18*). The difference in the effectiveness of IVIG on circulating mAb in mice versus humans may be related to the 8-fold higher binding affinity of the Fc receptor for mouse than for human IVIG or the relatively low dose of IVIG given to the subjects, as compared with the mice. Although larger amounts of IVIG might overcome this limitation, logistic considerations combined with the cost of IVIG prevented us from evaluating this possibility further.

TABLE 2
Pharmacokinetic Parameters Based on Well Counting

Pharmacokinetic parameter	Intravenous (n = 14)		IVIG (n = 5)		HAI (n = 6)	
	Mean ± SD	Median	Mean ± SD	Median	Mean ± SD	Median
Co (%ID/L)	31.9 ± 6.5		38.0 ± 9.7		29.7 ± 6.0	
$T_{1/2}$ (h)*	65.2 ± 9.8	63.9	41.6 ± 14.0*	41.7	65.2 ± 9.9	68.2
AUC (%ID × h/L)	3,330 ± 648	3,205	2,838 ± 699	2,772	2987 ± 808	2,825
Clearance (mL/h)	31.0 ± 5.6	31.2	36.8 ± 8.4	36.1	35.2 ± 8.0	35.7
Volume of central compartment (mL)	3,257 ± 631.2	3,221	2,758 ± 634	2,986	3,498 ± 603	3,505
Calculated plasma volume (mL)	2,992 ± 491.9	3,171	2,935 ± 370	2,950	3,100 ± 417	3,363

*IVIG $T_{1/2}$ shorter than intravenous or HAI is significantly different; all other values are not significantly different (Kruskal–Wallis 1-way ANOVA).

Co = estimated initial drug concentration in serum.

The targeting of huA33 to normal bowel has been a major concern for radioimmunotherapy or immunotherapy trials, although clinical trials have not shown toxicity (*6,9,10,32*). Prior studies using NR-LU-10 mAb, which cross-reacts with normal bowel, resulted in dose-limiting gastrointestinal toxicity when high amounts of ^{90}Y were used (*33*). Scott et al. developed a kinetic model for colonic uptake of huA33 and derived a mean colon $T_{1/2}$ of bowel activity of 32.4 h (*32*), suggesting that targeted activity in bowel may be exfoliated over time. We are currently exploring whether our quantitative PET data can be used to model the kinetics of bowel binding and whether the information can be used to optimize pretargeting approaches with respect to colon localization.

Despite the preferential localization in tumor relative to normal colon, some of the primary colon tumors and lymph node lesions were difficult to identify on PET/CT because of the adjacent high background activity. It is possible that with more delayed images, higher contrast would have been achieved, given prior studies that showed prolonged retention of activity in tumor up to 4–6 wk after tracer administration with clearance from bowel (*6,11*).

Although prior studies typically attributed activity in bowel to colonic activity, our PET studies with CT-based anatomic coregistration showed that the concentration of ^{124}I-huA33 appeared much higher in the small bowel than in the colon. Nevertheless, in 3 patients who underwent resection of the cecum, there was adjacent normal ileum, and its concentration was similar to that in normal colon (Table 1). It is possible that these differences between small-bowel and colon concentration detected on PET were related to partial-volume effects (*34*). Alternatively, we cannot completely exclude the possibility that the concentration in other segments, such as jejunum, may be different.

In all patients undergoing HAI, there was localization in liver metastases but no visual difference in the amount or timing of uptake by liver metastases between the HAI and the intravenous routes. Further, pharmacokinetic analysis demonstrated that HAI did not differ kinetically from intravenous administration. Delivery of antibodies from the vasculature to tumors depends on both diffusion and convection, and it is likely that given the large size of antibodies, these are slow processes that result in low first-pass extraction (*35*). The mild improvement that other studies have described for the HAI route may be related to differences in tumor vascularity and antigen access, because those studies were on patients with hepatoma (*21–23*).

CONCLUSION

^{124}I-huA33 was well tolerated and had favorable imaging properties, with high concentrations achieved in tumors. Although the high concentration in bowel limited the evaluation of primary disease and regional lymph nodes, there was excellent localization in liver tumors that might be useful in the evaluation of metastatic liver disease. Beyond determining the specifics of the distribution of ^{124}I-huA33, this work is significant for being among the first to confirm, against a gold standard (well counting of serum and tissues), that one can use ^{124}I to label antibodies and quantitatively evaluate their pharmacokinetics, biodistribution, and targeting.

DISCLOSURE STATEMENT

The costs of publication of this article were defrayed in part by the payment of page charges. Therefore, and solely to indicate this fact, this article is hereby marked "advertisement" in accordance with 18 USC section 1734.

ACKNOWLEDGMENTS

We thank Christina Hong, Ernest Flatts, and Christine Pierre for their research support; Amabella Lindo and Susan Reyes for their excellent nursing care; research chemist Jing Qiao for labeling the mAb; the nuclear medicine technologists and pharmacist for their technical assistance; and Franklin Torres for his editorial assistance. This research was supported by the Ludwig Institute for Immunotherapy, New York, New York, and by NCI grant P01 CA33049. No other potential conflict of interest relevant to this article was reported.

REFERENCES

1. Dougan M, Dranoff G. Immune therapy for cancer. *Annu Rev Immunol.* 2009;27:83–117.
2. Divgi CR, Pandit-Taskar N, Jungbluth AA, et al. Preoperative characterisation of clear-cell renal carcinoma using iodine-124-labelled antibody chimeric G250 (^{124}I-cG250) and PET in patients with renal masses: a phase I trial. *Lancet Oncol.* 2007;8:304–310.
3. Dijkers EC, Oude Munnink TH, Kosterink JG, et al. Biodistribution of ^{89}Zr-trastuzumab and PET imaging of HER2-positive lesions in patients with metastatic breast cancer. *Clin Pharmacol Ther.* 2010;87:586–592.
4. Sakamoto J, Kojima H, Kato J, Hamashima H, Suzuki H. Organ-specific expression of the intestinal epithelium-related antigen A33, a cell surface target for antibody-based imaging and treatment in gastrointestinal cancer. *Cancer Chemother Pharmacol.* 2000;46:S27–S32.
5. Ackerman ME, Chalouni C, Schmidt MM, et al. A33 antigen displays persistent surface expression. *Cancer Immunol Immunother.* 2008;57:1017–1027.
6. Welt S, Scott AM, Divgi CR, et al. Phase I/II study of iodine 125-labeled monoclonal antibody A33 in patients with advanced colon cancer. *J Clin Oncol.* 1996;14:1787–1797.
7. Welt S, Divgi CR, Real FX, et al. Quantitative-analysis of antibody localization in human metastatic colon cancer: a phase I study of monoclonal antibody A33. *J Clin Oncol.* 1990;8:1894–1906.
8. Welt S, Divgi CR, Kemeny N, et al. Phase I/II study of iodine 131-labeled monoclonal-antibody A33 in patients with advanced colon-cancer. *J Clin Oncol.* 1994;12:1561–1571.
9. Welt S, Ritter G, Williams C, et al. Preliminary report of a phase I study of combination chemotherapy and humanized A33 antibody immunotherapy in patients with advanced colorectal cancer. *Clin Cancer Res.* 2003;9:1347–1353.
10. Welt S, Ritter G, Williams C, et al. Phase I study of anticolon cancer humanized antibody A33. *Clin Cancer Res.* 2003;9:1338–1346.
11. Chong G, Lee F, Hopkins W, et al. Phase I trial of ^{131}I-huA33 in patients with advanced colorectal carcinoma. *Clin Cancer Res.* 2005;11:4818–4826.
12. Sakamoto J, Oriuchi N, Mochiki E, et al. A phase I radioimmunolocalization trial of humanized monoclonal antibody huA33 in patients with gastric carcinoma. *Cancer Sci.* 2006;97:1248–1254.
13. Welt S, Divgi CR, Scott AM, et al. Antibody targeting in metastatic colon-cancer: a phase I study of monoclonal-antibody F19 against a cell-surface protein of reactive tumor stromal fibroblasts. *J Clin Oncol.* 1994;12:1193–1203.

14. Goodwin D, Meares C, Diamanti C, et al. Use of specific antibody for rapid clearance of circulating blood background from radiolabeled tumor imaging proteins. *Eur J Nucl Med.* 1984;9:209–215.
15. Axworthy DB, Reno JM, Hylarides MD, et al. Cure of human carcinoma xenografts by a single dose of pretargeted yttrium-90 with negligible toxicity. *Proc Natl Acad Sci USA.* 2000;97:1802–1807.
16. Lear JL, Kasliwal RK, Feyerabend AJ, et al. Improved tumor imaging with radiolabeled monoclonal-antibodies by plasma-clearance of unbound antibody with anti-antibody column. *Radiology.* 1991;179:509–512.
17. Telleman P, Junghans RP. The role of the Brambell receptor (FcRB) in liver: protection of endocytosed immunoglobulin G (IgG) from catabolism in hepatocytes rather than transport of IgG to bile. *Immunology.* 2000;100:245–251.
18. Jaggi JS, Carrasquillo JA, Seshan SV, et al. Improved tumor imaging and therapy via i.v. IgG-mediated time-sequential modulation of neonatal Fc receptor. *J Clin Invest.* 2007;117:2422–2430.
19. Moseley RP, Benjamin JC, Ashpole RD, et al. Carcinomatous meningitis: antibody-guided therapy with I-131 HMFG1. *J Neurol Neurosurg Psychiatry.* 1991;54:260–265.
20. Stewart JSW, Hird V, Snook D, et al. Intraperitoneal radioimmunotherapy for ovarian-cancer: pharmacokinetics, toxicity, and efficacy of I-131 labeled monoclonal-antibodies. *Int J Radiat Oncol Biol Phys.* 1989;16:405–413.
21. Fan Z, Tang ZY, Liu KD, et al. Radioiodinated anti-hepatocellular carcinoma (HCC) ferritin: targeting therapy, tumor imaging and anti-antibody response in HCC patients with hepatic arterial infusion. *J Cancer Res Clin Oncol.* 1992;118:371–376.
22. Chen ZN, Mi L, Xu J, et al. Targeting radioimmunotherapy of hepatocellular carcinoma with iodine (^{131}I) metuximab injection: clinical phase I/II trials. *Int J Radiat Oncol Biol Phys.* 2006;65:435–444.
23. Zeng ZC, Tang ZY, Liu KD, Lu JZ, Xie H, Yao Z. Improved long-term survival for unresectable hepatocellular carcinoma (HCC) with a combination of surgery and intrahepatic arterial infusion of ^{131}I-anti-HCC Mab: phase I/II clinical trials. *J Cancer Res Clin Oncol.* 1998;124:275–280.
24. King DJ, Antoniw P, Owens RJ, et al. Preparation and preclinical evaluation of humanized A33 immunoconjugates for radioimmunotherapy. *Br J Cancer.* 1995;72:1364–1372.
25. Lee YS, Bullard DE, Wikstrand CJ, Zalutsky MR, Muhlbaier LH, Bigner DD. Comparison of monoclonal-antibody delivery to intracranial glioma xenografts by intravenous and intracarotid administration. *Cancer Res.* 1987;47:1941–1946.
26. Day ED, Lassiter S, Woodhall B, Mahaley JL, Mahaley MS. Localization of radioantibodies in human brain tumors. I. Preliminary exploration. *Cancer Res.* 1965;25:773–778.
27. Barendswaard EC, Scott AM, Divgi CR, et al. Rapid and specific targeting of monoclonal antibody A33 to a colon cancer xenograft in nude mice. *Int J Oncol.* 1998;12:45–53.
28. Heath JK, White SJ, Johnstone CN, et al. The human A33 antigen is a transmembrane glycoprotein and a novel member of the immunoglobulin superfamily. *Proc Natl Acad Sci USA.* 1997;94:469–474.
29. Lindmo T, Boven E, Cuttitta F, Fedorko J, Bunn PA. Determination of the immunoreactive fraction of radiolabeled monoclonal-antibodies by linear extrapolation to binding at infinite antigen excess. *J Immunol Methods.* 1984; 72:77–89.
30. Common Toxicity Criteria, Version 2.0. National Cancer Institute Web site. Available at: http://ctep.cancer.gov/protocoldevelopment/electronic_applications/docs/ctcv20_4-30-992.pdf. Published April 30, 1999. Revised March 23, 1998. Accessed June 7, 2011.
31. Ritter G, Cohen LS, Williams C, Richards EC, Old LJ, Welt S. Serological analysis of human anti-human antibody responses in colon cancer patients treated with repeated doses of humanized monoclonal antibody A33. *Cancer Res.* 2001;61:6851–6859.
32. Scott AM, Lee FT, Jones R, et al. A phase I trial of humanized monoclonal antibody A33 in patients with colorectal carcinoma: biodistribution, pharmacokinetics, and quantitative tumor uptake. *Clin Cancer Res.* 2005;11:4810–4817.
33. Knox SJ, Goris ML, Tempero M, et al. Phase II trial of yttrium-90-DOTA-biotin pretargeted by NR-LU-10 antibody/streptavidin in patients with metastatic colon cancer. *Clin Cancer Res.* 2000;6:406–414.
34. Hoetjes NJ, van Velden FHP, Hoekstra OS, et al. Partial volume correction strategies for quantitative FDG PET in oncology. *Eur J Nucl Med Mol Imaging.* 2010;37:1679–1687.
35. Jain RK. Transport of molecules in the tumor interstitium: a review. *Cancer Res.* 1987;47:3039–3051.